Analysis of tile-substrate behavior subjected to shrinkage

Gian Piero Lignola[1], Amilcare Collina[2], Andrea Prota[1], Gaetano Manfredi[1]

[1]*Department of Structural Engineering, University of Naples "Federico II", Italy*
E-mail: *glignola@unina.it, aprota@unina.it, gamanfre@unina.it*

[2]*MAPEI S.p.A., Milan, Italy*
E-mail: *a.collina@mapei.it*

Keywords: Tiles, Adhesive, Shrinkage.

SUMMARY. The aim of this paper is to analyze the behavior of tile-substrate adhesive joints in tiled flooring. A refined Finite Element Model (F.E.M.) has been developed to analyze the stress and strain distributions in a tile-adhesive-substrate system without spacers and tile grout joints.
The brittle behavior of such composite structural system is examined considering the interaction between the shear and normal stresses due to the bonding system. The modeling assumes linear behavior for the materials and connection, and it allows different structural problems to be analyzed for any given tiling configuration. The model has been validated by means of experimental tests on 18 specimens reproducing tiled floorings, the key issue is that the restrained shrinkage causes a deflection in the system, thus leading to a fully 2D problem.

1 INTRODUCTION

The substrate shrinkage, related to thermal gradients or maturation of the cementitious substrate, causes compression of the tiles because the adhesive transfers the stresses induced by the constrained deformation through shearing. The aim of the present work is to provide the end user with a tool for the selection of the most appropriate adhesive, in terms of stiffness, strength and thickness for a given tile and substrate system. Furthermore, the F.E.M. analyses demonstrated that a statically equivalent axial compression force can effectively simulate the shrinkage effect, complex to be simulated otherwise in the lab. This consideration allowed to design a specific experimental program to analyze the effects of shrinkage on a tile-adhesive-substrate system.

A previous work [1] analyzed the compression force in the tiles promoting Mode I decohesion of the tiles due to out-of-plane type defects, taking into account the presence of grout joints. Random defects generate a bending moment at the tile edge which acts as driving force for decohesion. A mode II shear mechanism was analyzed also by means of a shear-lag model for the transmission of the shear stress produced by the substrate shrinkage and by means of a F.E.M. analysis. Both analyses assumed the substrate constrained in the vertical direction (and the results were in very good agreement), then Mode I mechanism was described through a cohesive interface. The tiles were loaded by a couple given by the compression force applied at an offset with respect to the tile’s mid-line (defect assumed for instance equal to 4 mm) leading to reasonable critical elastic normal strength for commercial adhesives. The valuable approach proposed [1] led to very simple closed formulas but they related the failure mechanism to a random defect. Apart from the boundary of the tiled flooring (where tangential stress in adhesive is higher), the stress state is almost equal in each tile of the flooring, and almost independently on the tile’s length. These models led to the conclusion that the failure of the tiles likely occurs at the boundary of flooring if shear failure is assumed or wherever on the floor if a failure mode related to random defects is assumed, while the experience shows that the failures, if any, systematically occur close to the mid-span of the floor, and tile's length is critical.

2 ANALYTICAL SOLUTIONS

Tile-adhesive-substrate systems can be considered as composite systems: they are very common in structural engineering to optimize the performance of the components [2]. Typical cases are steel-concrete composite beams, where steel beams and concrete slabs are connected by mechanical devices to improve the performances of both materials. Another example of system is coupled shear walls particularly suitable for resisting horizontal loads. A further composite system is given by Reinforced Concrete beams externally reinforced with laminates or sheets for strengthening existing structures by means of fiber reinforced plastic (FRP). Also for this problem, linear models accounting for both axial and shear stresses have been developed but two main important issues came out: (i) in the external strengthening the applied loads determine the stress and strain distributions in the substrate, while in the present case the strains and stresses are due to the constrained shrinkage - a distortion -, (ii) the FRP laminates externally applied to the beams or to other structural members present small thicknesses and hence reduced flexural and axial stiffness, and it is not the case of the tiles, presenting significant stiffness. It is worth noted that the higher is the stiffness of the tiles, the higher are the stresses induced in the entire system. This is due to the constrained deformations.

Furthermore the models proposed for the externally bonded reinforcements are based on the solution of complex high order differential equations which need the definition of precise boundary conditions related to both equilibrium and compatibility at the joints between tiles and between the tiles and the substrate through the adhesive layer.

3 F.E.M. MODELING

The application of analytical models is jeopardized by the relevant uncertainty on the boundary conditions to be inserted in such models thus providing further and higher uncertainties on the predictions of these models. This is the primary reason for which the authors selected the F.E.M. as the best tool approaching such class of problems, otherwise analyzed by means of very refined models, but driven by tricky boundary assumptions at the tile joints and between the tiles and the substrate because of the adhesive layer.

Preliminary experimental tests showed that the restrained shrinkage causes a deflection in the system, thus decisively leading to a fully 2D problem, where the vertical displacement is only restrained at the two edges of the flooring acting as simple supports on the underlying structure. TNO DIANA v9.1 [3] code was adopted to perform the analyses. Linear elastic behavior was assumed for all the materials, plane stress was assumed to perform 2D analyses. A typical flooring system about 4.8 m long (thickness 40 mm) was analyzed, whole tiles with dimensions of 600 mm and 300 mm (thickness 8 mm) were placed on 3 mm adhesive layer. Three different adhesives were considered. The model presents more than 10,000 elements allowing average element dimensions being about 5 mm. The geometry of the flooring is depicted in Figure 1.

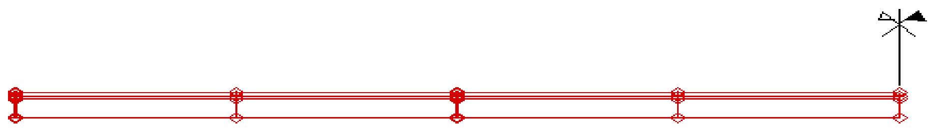

Figure 1: Geometry of the model reproducing half tiled flooring.

Material	Young Modulus E	Shear Modulus G	Poisson's Coefficient ν	Density γ	Peeling Strength (EN 1348)
Tile	50.0 GPa	20.8 GPa	0.200	22 kN/m^3	*n.a.*
Adhesive 1	8.0 GPa	3.4 GPa	0.175	15 kN/m^3	1.0 MPa
Adhesive 2	7.0 GPa	2.5 GPa	0.400	15 kN/m^3	2.0 MPa
Adhesive 3	3.5 GPa	1.3 GPa	0.300	15 kN/m^3	2.5 MPa
Substrate	22.0 GPa	9.4 GPa	0.175	25 kN/m^3	*n.a.*

Table 1: Mechanical properties of the involved materials.

The loads on the system are the self-weight and the substrate shrinkage assumed equal to 400 μm/m. The adhesive layer was modeled by means of special CL12I interface elements (3+3 nodes) with normal and transversal stiffness E/t_a e G/t_a, where t_a is the thickness of the adhesive. Substrate and tiles were modeled by means of 8 nodes CQ16M plane stress elements. Mechanical properties for all the involved materials are reported in Table 1. Adhesive 1 is a normal mono-component cementitious adhesive, while adhesive 2 is a deformable mono-component cementitious adhesive. Adhesive 3 is a bi-component cement based adhesive with latex additive to improve adhesion and deformability.

Figure 2 shows the deformed shape of the system bending after shrinkage took place.

Figure 2: Deformed shape of the model reproducing half tiled floor.

In Figure 3a is depicted the normal (traction is negative) and transverse stress diagram for the adhesive layer in the case of 600 mm tiles applied with adhesive 2. It is clearly highlighted the increasing normal stress moving from the boundary (abscissa 0) of the floor to the center (abscissa 2400); conversely the shear stresses reduce. Figure 3b clearly shows that the normal stresses are associated to shear stresses thus leading to severe stress conditions as indicated in the σ/τ plane. For the sake of simplicity, in the following, the failure due to peeling only will be considered, but such σ/τ coupling demonstrates that the failure of the adhesive can be triggered for normal stresses lower than peeling strengths reported in Table 1.

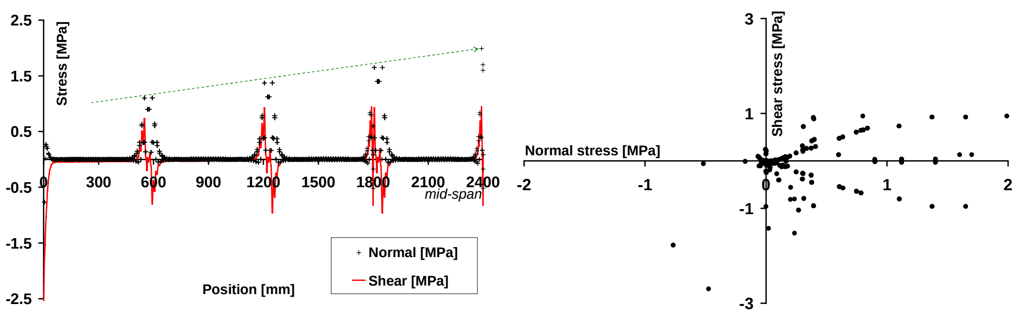

a) b)

Figure 3: Stress state in the adhesive: a) diagram along half flooring, b) in the σ/τ plane.

The F.E.M. analyses highlighted also the extreme influence of the detail of the tile joints on the strength predictions of the adhesive. Three different geometrical layouts were considered for the contact area, each of them assuming four values for the contact dimension B (0.5 mm - 1 mm - 2 mm - 4 mm). In Figure 4 the details considered for the contact area are depicted (where obviously A+B+C = 8 mm, the thickness of a tile).

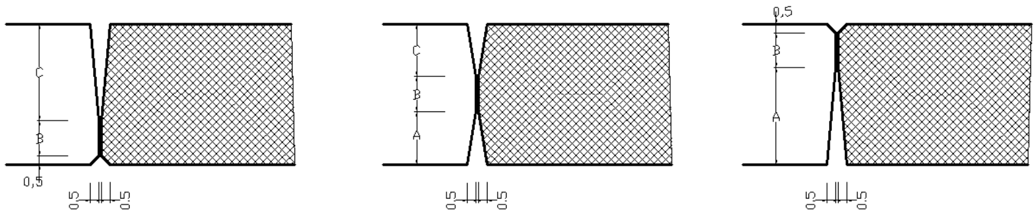

Figure 4: Details of the contact area and the shapes of the tile joints adopted in the analyses.

The main outcomes of the analyses with the lower contact area (considered in the following as the most realistic case) are summarized in Figures 5. Figure 5a and 5b highlight the influence of the contact area dimensions and the tile's length, respectively, on the peak normal tensile stresses (peeling) in the adhesive layer. A punctual contact area (B<0.5 mm) provides peak stresses not depending on the tile's length.

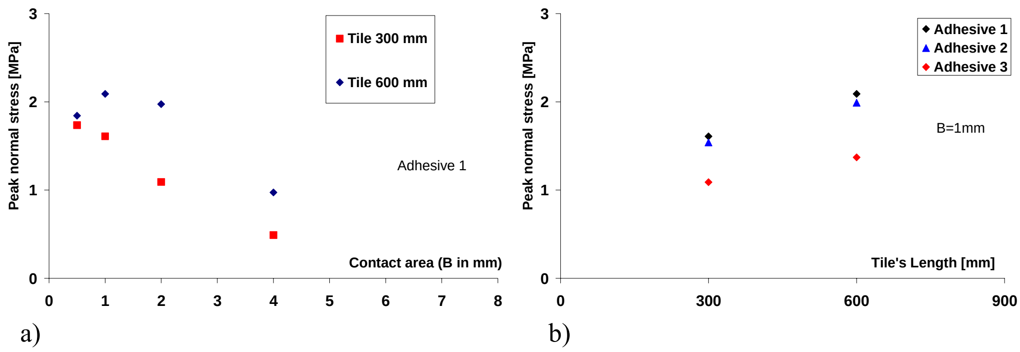

Figure 5: Peak normal stress in the adhesive vs.: a) Contact area dimension, b) Tile's length.

Analyses clearly showed that the adhesive is stressed only close to the edges of each tile: the portion loaded by shear and normal stresses is only about 50 mm long. Nevertheless the coupled stresses σ/τ could attain values higher than the adhesive strength thus causing the failure of the system.

If the peak tensile stresses in the adhesive are compared with the peeling strengths, it is clear that the analyses predict failure for the tiles with the stiffest adhesive 1, safety conditions for the shortest tile with adhesive 2 and incipient failure for the longest tile having a peak stress very close to peeling strength. The tiles with the bi-component adhesive 3 present a safety factor (capacity over demand ratio) of about 2.

3.1 *Remarks on the F.E.M. modeling*

1) Boundary conditions between each tile along the floor are crucial to evaluate normal and shear stresses.

2) Peak stress in the adhesive (normal peeling stress) is in tension and it occurs in the central tile (stress increasing from the boundary edges to the middle of the floor), the opposite is found in the case of shear stresses.

3) Tiles and contact area between tiles are always in compression (horizontal direction).

4) For the same adhesive, stresses increase when tile's length and floor's dimensions increase; they reduce when the adhesive exhibit lower stiffness.

5) Curvature in the substrate is usually different if compared to the curvature of the tiles (analytical closed-form models can be easily developed assuming they are equal, but leading to inaccurate predictions).

6) At the edges of each tile there are both normal and shear stresses. So there is an interaction between the two stress components, that was shown in Figure 3b in the σ/τ plane. A detailed characterization of adhesives is needed to take into account this remark.

7) Deformed shape of the system can be approximated with a polynomial (degree 4), thus the curvature in the substrate is not constant.

4 THE EXPERIMENTAL PROGRAM

Preliminary F.E.M. analyses demonstrated that a statically equivalent axial compression force can effectively simulate the shrinkage effect. The experimental program allowed also to validate the F.E.M. analyses, and main parameters driving the behavior of such systems have been pointed out. The test setup is depicted in Figures 6: the three adhesives and the two tile's lengths were tested, and each of the six combinations (see Table 2) was repeated three times. The design of the test matrix required particular attention because there was the need to validate the numerical analyses by means of clear predictions of failure or safety to be compared to the tested experimental systems. Furthermore there was the need to test sufficiently large-scale specimens to be representative of the real situations however avoiding premature failures due to stability or punching or accidental eccentricities.

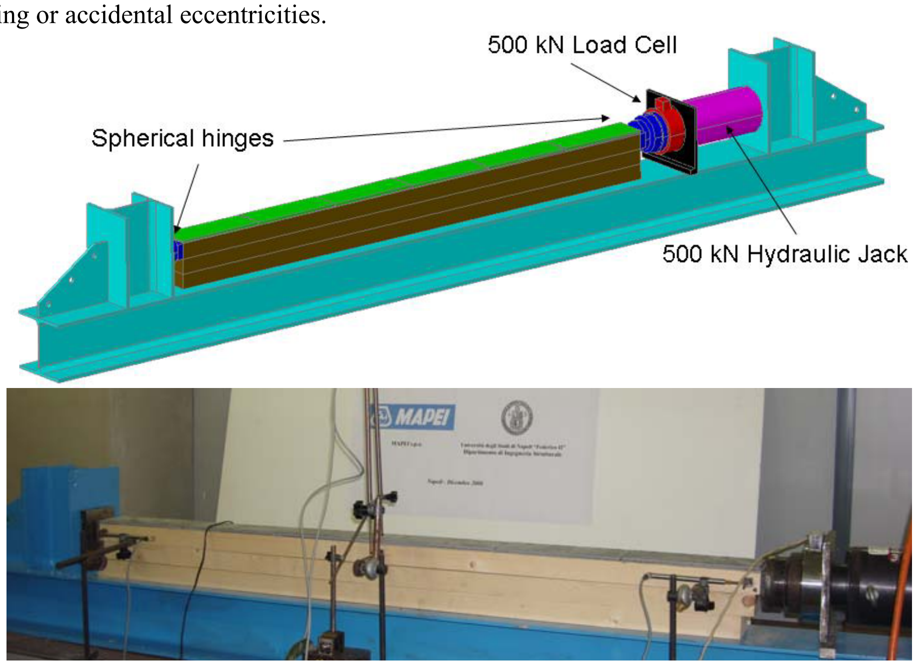

Figure 6: Test setup and a tested specimen reproducing tiled flooring.

An experimental program has been conducted on 18 specimens (6 triplets) reproducing tiled floorings at the University of Naples “Federico II”. The application of a direct shrinkage load was avoided due to the time consumption and difficulties in terms of temperature and humidity control. The application of a compression axial force on a slender system as a tiled floor needs the test setup and test matrix to be carefully designed because of stability and punching problems. F.E.M. analyses provided the compression force value to simulate the shrinkage: only at the boundary edges of the flooring some deviations were found in the stress state of the substrate, but they expire very close to the two edges. Furthermore it is noted that the length of the floor has a key role on the failure of the adhesive, but the specimens cannot have the real length (about 5 meters) due to slenderness issues. Thus a different material was adopted for the substrate: it was made of timber: compared to a cementitous substrate it is less brittle and easier to handle in the laboratory. The Young Modulus E of the timber is approximately halved (it is assumed equal to 11.0 GPa) and for this reason substrate’s thickness was increased up to 50 mm to provide almost the same flexural stiffness *EI*, crucial parameter for the stress state in the adhesive layer. The length of the flooring is assumed equal to 1.8 m allowing the placement of six 300 mm tiles or twelve 150 mm tiles, respectively: the length is limited to reduce stability issues and correspondingly the length of the tiles was reduced to scale the effective geometry of real flooring systems. The specimen’s dimensions are reported in Figure 7. The horizontal load and displacement and the deflection at mid-span were measured.

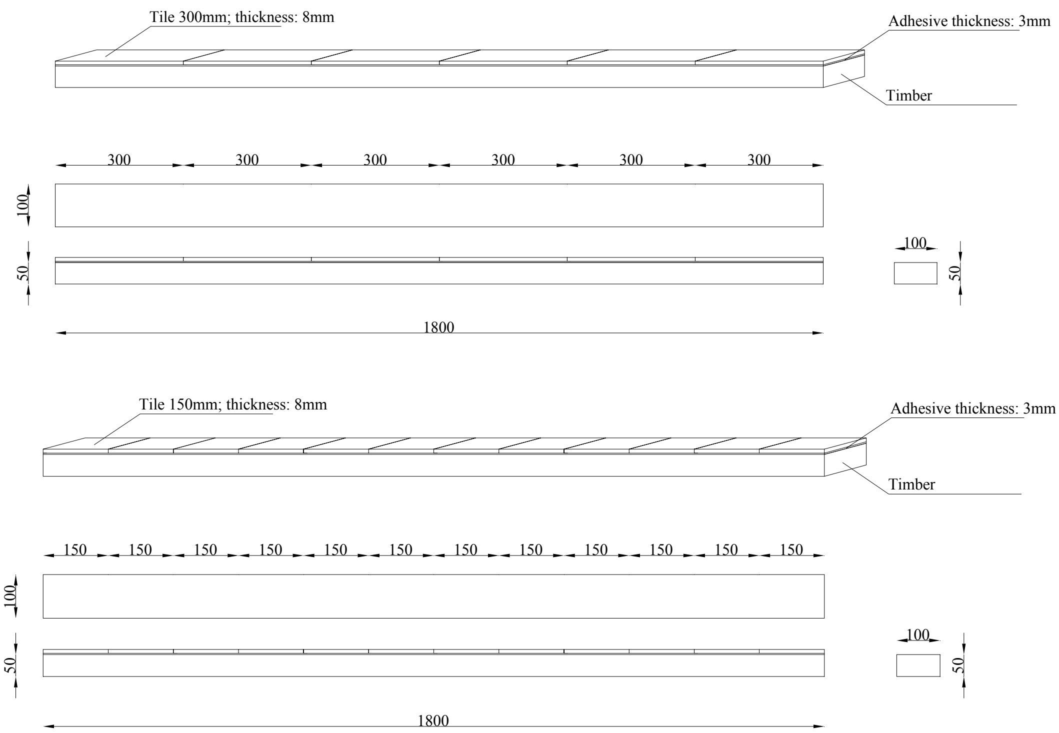

Figure 7: Dimensions of the tested specimens.

It was possible to predict numerically the peak tensile stresses in the adhesive layer for the six combinations (see Figure 8), comparing them to the effective peeling strengths: these values– 0.40 MPa; 1.00 MPa and 1.75 MPa respectively for adhesive 1; 2 and 3- are lower than those reported in Table 1 for traditional cementitious substrates, because the same adhesives presented lower adhesion with timber substrate during specific pull-out tests.

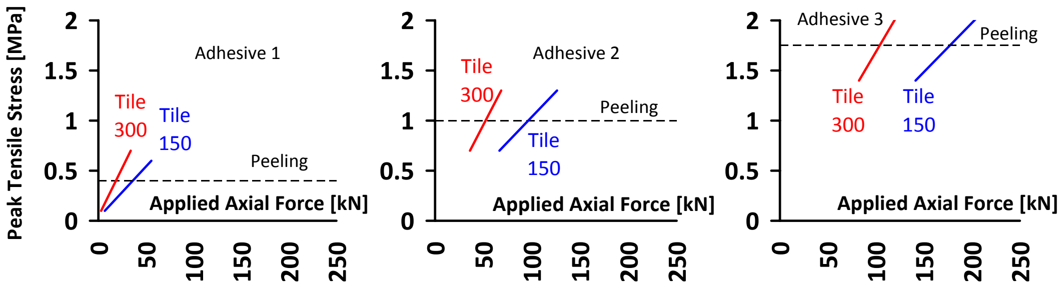

Figure 8: F.E.M. predictions of peak tensile stresses in the adhesive layer vs. axial force: six tile/adhesive combinations and comparison with peeling strengths.

4.1 *Remarks on the Experimental Program and Numerical/experimental comparisons*

The rationale is to validate the F.E.M. predictions in the case of an axial force of about 50 kN applied on the specimens and equal for each test (corresponding to about two times the design shrinkage), thus simulating conditions similar to those reported in Figure 5b for real tiled floors:

1) failure for all the tiles with adhesive 1 and for the longest tile with adhesive 2;

2) safety conditions for the shortest tile with adhesive 2 and for all the tiles with adhesive 3.

This test matrix is summarized in Table 2 with the experimental/numerical comparisons: it can be easily checked that the F.E.M. model is validated (in the numerical analyses a contact area characterized by B=1 mm was assumed, and the peak stresses correspond to average experimental axial force for each triplet).

Tile's Length	Adhesive #	Experim. Force (Ave.)	F.E.M. peak tensile stress	Peeling Strength	Observed Failure mode
300 mm	1	45 kN	0.90 MPa	0.40 MPa	Middle: tiles detachment
150 mm		44 kN	0.48 MPa		Middle: Adhesive fracture
300 mm	2	52 kN	1.00 MPa	1.00 MPa	Middle: tiles detachment
150 mm		49 kN	0.52 MPa		None *(substrate stability)*
300 mm	3	51 kN	0.89 MPa	1.75 MPa	None *(substrate stability)*
150 mm		45 kN	0.46 MPa		None *(substrate stability)*

Table 2: Six tile/adhesive combinations and experimental/numerical comparisons.

Despite the stability issues occurred due to the slenderness of the specimens, it was possible to numerically simulate the behavior of the specimens: failure was correctly predicted (peak tensile stress, at mid-span, higher than corresponding peeling strength) for the first three specimens reported in Table 2 showing a detachment failure mode at mid-span of the floor or adhesive fracture (same failure mode for each specimen of the triplets).

Figure 9: 300 mm tiles and adhesive 3: deflection higher than 50 mm.

The remaining specimens had no detachments according also to the numerical predictions presenting a safety factor of about 2. It was very impressive the behavior of specimens with adhesive 3 showing relevant bending with a displacement higher than 50 mm not accompanied by any failure of the adhesive (see Figure 9).

Stability issues limited the axial load not allowing the failure to be achieved for the latter specimens (the F.E.M. failure load prediction in these cases is higher than about 100 kN). The maximum experimental load was always, even if slightly, higher in the case of longer tiles. This is compatible with F.E.M. analyses systematically predicting smaller displacements in that case: higher transverse displacements trigger stability issues later, thus for higher loads.

Typical load vs. horizontal displacement and vertical displacement at mid-span are reported in Figures 10 and 11, respectively, for 150 mm and 300 mm tiles in the case of adhesive 1. The dashed lines represent the F.E.M. elastic predictions, the deviation of the experimental solid lines is basically related to P-Delta effects in slender compressed members and to the nonlinear behavior of timber. However first elastic branch of the curves is satisfactorily predicted by F.E.M.

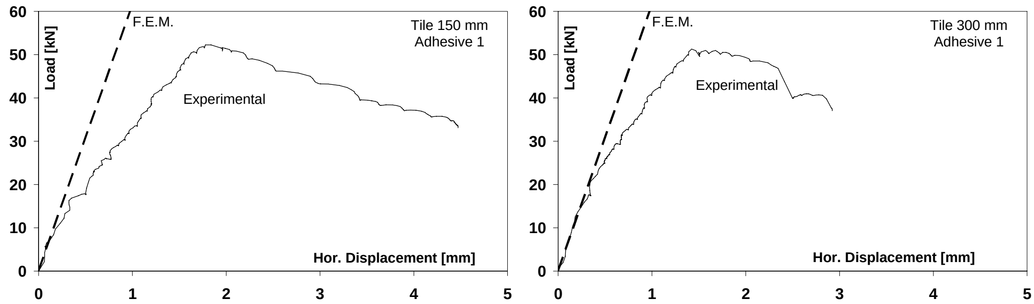

Figure 10: Axial load vs. horizontal displacement diagram.

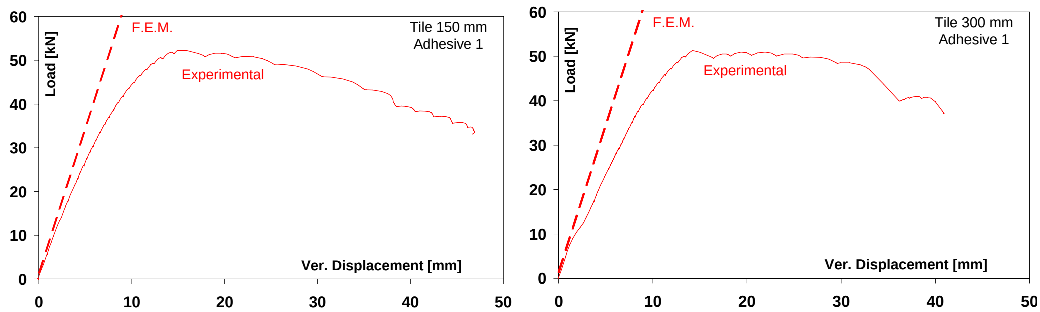

Figure 11: Axial load vs. vertical displacement at mid-span diagram.

Pictures of the failed tiles clearly show in Figure 12 a fracture of the adhesive: the tile lifted up totally detaching (a footstep would have certainly cracked the tile), while in Figure 13 there is an incipient detachment: a zoom on the adhesive layer clearly shows the cracking of the adhesive along an horizontal line. In a real flooring this last failure mode would clearly have originated a complete detachment. It is highlighted that for the specimens not showing any failure (e.g. with adhesive 3), despite the large deflection at the maximum axial load, the scalpel was needed to attempt detaching the tiles after the tests.

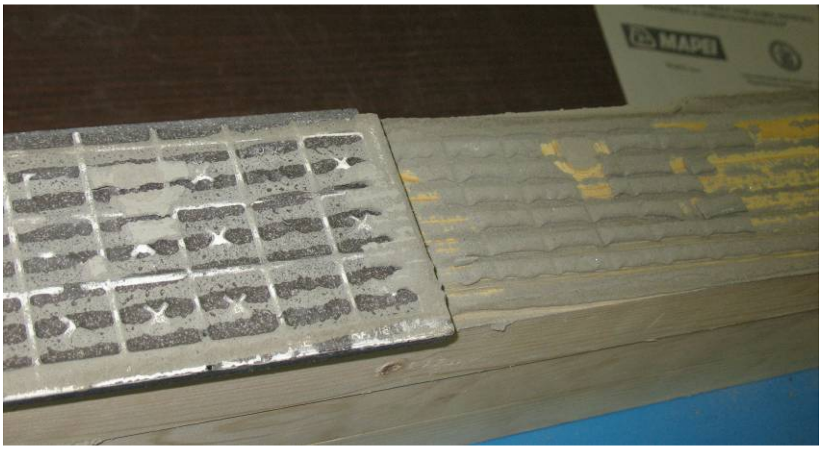

Figure 12: Mixed fracture of the adhesive (the tile was manually overturned at the end of the test).


Figure 13: Cracking of the adhesive along an horizontal line.

5 CONCLUSIONS

Based on the outcomes of the experimental program, the restrained shrinkage causes a deflection in the system, thus leading to a fully 2D problem: this is a key aspect of the present work. The estimation of the compression force in the tiles and the stress in the adhesive is strictly related to the development of curvatures inside the substrate. The failure, according also to previous knowledge of failed tiled floors, occurs in the middle of the system where the adhesive is almost subjected to normal vertical stresses rather than shear stresses.

The F.E.M. analyses, validated by means of 18 experimental tests, highlighted the extreme influence of the detail of the tile contact area on the predictions of peak stress demand in the adhesive (mostly at mid-span of the flooring). In this sense the application of analytical models is jeopardized by the relevant uncertainty on those boundary conditions to be inserted in such models thus providing further and higher uncertainties on the predictions of these models.

The sensitivity in F.E.M. to the main parameters driving the behavior of such systems have been highlighted, namely: the dimensions of the tiles compared to the average in plane dimensions of the substrate/floor, the pull-out strength and the stiffness of the adhesive, the shear strength compared to the pull-out strength of the adhesive, the flexural stiffness of the tiles compared to the substrate counterpart, the contact area and the shape of the tile joints detail.

The proposed modeling, experimentally validated, was able to predict the failure that, if any, can occur at mid-span of the floors, being longer tiles and stiffer adhesives more critical. This model hence is a valid tool to support the selection of the most appropriate adhesive considering the effective geometrical and mechanical properties of the components of the system. Furthermore it can be adopted to design new materials with optimized cost/performance ratios.

The experimental program, despite the great difficulties in providing sufficiently large scale specimens still avoiding stability limits and reproducing realistic conditions of failure, or not, for different adhesives, was crucial to understand the 2D behavior of tile-substrate systems.

References

[1] Cocchetti G., Comi C. and Perego U., "A simplified assessment of bonding strength in tiled flooring",. in *Proc. XVIII Congresso Associazione Italiana di Meccanica Teorica e Applicata* (Aimeta 2007 Conference Proceedings, Starrylink, 2007), Brescia, Italy, September 11-14, 608pp. (2007).

[2] Fabbrocino G., Manfredi G. and Cosenza E., "Modelling of continuous steel-concrete composite beams: computational aspects", *Computer and Structures*, **80**, 2241-2251 (2002).

[3] De Witte, F.C. and Kikstra, W.P. *DIANA 9. Finite Element Analysis. User's Manual. Analysis Procedures*, TNO DIANA bv, Delft, The Netherlands (2005).